Conjugated Chitosan as a Novel Platform for Oral Delivery of Paclitaxel

Eunhye Lee,[†] Jinju Lee,[†] In-Hyun Lee,[†] Mikyung Yu,[†] Hyungjun Kim,[†] Su Young Chae,[‡] and Sangyong Jon*[,†,×]

Cell Dynamics Research Center, Department of Life Science, Gwangju Institute of Science and Technology (GIST), 1 Oryong-dong, Gwangju 500−712, South Korea, College of Pharmacy, SungKyunKwan University, 300 Chenchen-dong, Suwon, South Korea, and AnyGen Corp., Gwangju TechnoPark, Daechon-dong, Gwangju 500-706, South Korea

Received June 23, 2008

A new platform for oral delivery of paclitaxel (PTX) was developed through chemical conjugation of PTX to a low molecular weight chitosan (LMWC). The LMWC-PTX conjugate contained ∼12 wt % PTX and showed greatly enhanced water solubility (>1 mg/mL) as compared to native PTX. The conjugate showed comparable IC_{50} values to that of the parent PTX against human cancer cell lines. The pharmacokinetic data revealed ∼42% of bioavailability after oral administration of 5 mg PTX/kg of the conjugate. When the conjugate (10 mg/kg based on PTX content) was administered orally to mice bearing xenograft or allograft tumors, the conjugate-treated group showed significant inhibition of tumor growth, which was comparable to that seen with PTX of the clinically available injected form, formulated in cremophor EL/ethanol (iv) but with much lower toxicity. Tracking I^{125}-labeled conjugate showed that LMWC-PTX was likely to be absorbed mainly from the ileum and reach the blood as the intact conjugate.

Introduction

Paclitaxel (PTX[a]) has shown promise as an effective antineoplastic agent against a broad spectrum of human malignancies, including breast and ovarian cancers.[1,2] But because of its extremely poor aqueous solubility, the most widely used form of PTX is formulated in a vesicle containing ethanol and cremophor EL. When administered by intravenous (iv) infusion, this formulation frequently triggers acute hypersensitivity reactions, characterized by dyspnea, flushing, rash, chest pain, tachycardia, hypotension, angioedema, and generalized urticaria.[3] In addition, this formulation contributes substantially to the nonlinear pharmacokinetic behavior of PTX observed in humans.[4] It would thus be highly desirable to develop an improved delivery platform for PTX that could, perhaps, also be used for other poorly water-soluble drugs.

Various attempts have been made to overcome the drawbacks of current PTX therapy. These have included developing a micellular formulation,[5−12] conjugation with water-soluble macromolecules,[13−18] and prodrug approaches.[19−24] With these efforts, moreover, an increasing amount of research has focused on development of an oral delivery system for PTX. Oral administration is the preferred regimen for treatment of chronic diseases such as cancer because it is convenient for patients and it eliminates the need to frequently visit a hospital for intravenous infusion.[25] A PTX formulation suitable for oral administration has not been available in large part because the overexpression of P-glycoprotein (P-gp) in gastrointestinal (GI) epithelial cells and first-pass metabolism by CYP450-dependent enzymes in the GI tract and liver severely limit the drug's bioavailability.[26] Nonetheless, several recently reported approaches appear promising in terms of increasing the oral bioavailability of PTX to clinically useful levels.[27−29] One approach is based on the concomitant use of PTX and P-gp inhibitors such as cyclosporine A and Valspodar, which greatly enhances bioavailability and is currently in clinical study.[27,30] Despite these promising results, there is a concern about the potential side effects of P-gp inhibitors, in that P-gp is known to protect the GI tract, brain, and excretory organs from xenotoxins and drugs.[31]

Chitosan has been widely used in the pharmaceutical field because it is known to be biocompatible, biodegradable, mucoadhesive, and nontoxic.[32,33] In addition, low molecular weight chitosan (LMWC) has recently emerged with even more favorable characteristics than the conventional high molecular weight equivalents (HMWC), including greater water solubility, lower toxicity, and a narrower molecular weight distribution.[34] What's more, one recent study showed that LMWC (average MW < 10 kDa) could reversibly open the tight junctions between intestinal epithelial cells in a Caco-2 cell model and that subsequent recovery of initial levels of transepithelial resistance was much faster than was seen with HMWC.[34] This ability of LMWC to quickly and reversibly open tight junctions could be a useful characteristic for a carrier of drug molecules, especially for oral delivery.

Herein we describe a LMWC-based conjugate system developed as a new delivery platform for hydrophobic anticancer drugs, especially PTX. Several favorable characteristics are anticipated with this conjugate system: (1) improved water solubility of PTX due to the presence of chitosan; (2) prolonged retention of the conjugate in the GI tract due to the mucoadhesive property of chitosan, which could result in enhanced overall uptake; (3) an ability to bypass the P-gp-mediated barrier (efflux pump), as the opening of tight junctions may enable the conjugate to be transported via a paracellular pathway; and (4) an ability to bypass CYP450-dependent metabolism because, once conjugated, PTX will no longer be a substrate of those enzymes. In addition, it is noteworthy that the conjugate is designed to release parent PTX through cleavage of a linker under physiological conditions[35] so that the conjugate can be considered to be a prodrug. Furthermore, we used LMWC with

* To whom correspondence should be addressed. Phone: + 82 62 970 2504. Fax: + 82 62 970 2484. E-mail: syjon@gist.ac.kr.
[†] Gwangju Institute of Science and Technology.
[×] AnyGen Corp.
[‡] SungKyunKwan University.

[a] Abbreviations: BHR, Bolton−Hunter reagent; CYP, cytochrome; DMF, *N*,*N*-dimethylformamide; EDC, 1-ethyl-3-(3-dimethylaminopropyl) carbodiimide hydrochloride; GI, gastrointestinal; HMWC, high molecular weight chitosan; iv, intravenous; LMWC, low molecular weight chitosan; NHS, *N*-hydroxysuccinimide; P-gp, P-glycoprotein; po, per oral; PTX, paclitaxel; SGF, simulated gastric fluid; SIF, simulated intestinal fluid.

10.1021/jm800767c CCC: $40.75
Published on Web 10/01/2008

Scheme 1. Schematic Diagram (A) and Synthetic Scheme (B) of LMWC-PTX; Arrow Indicates the Cleavable Bond between LMWC and PTX

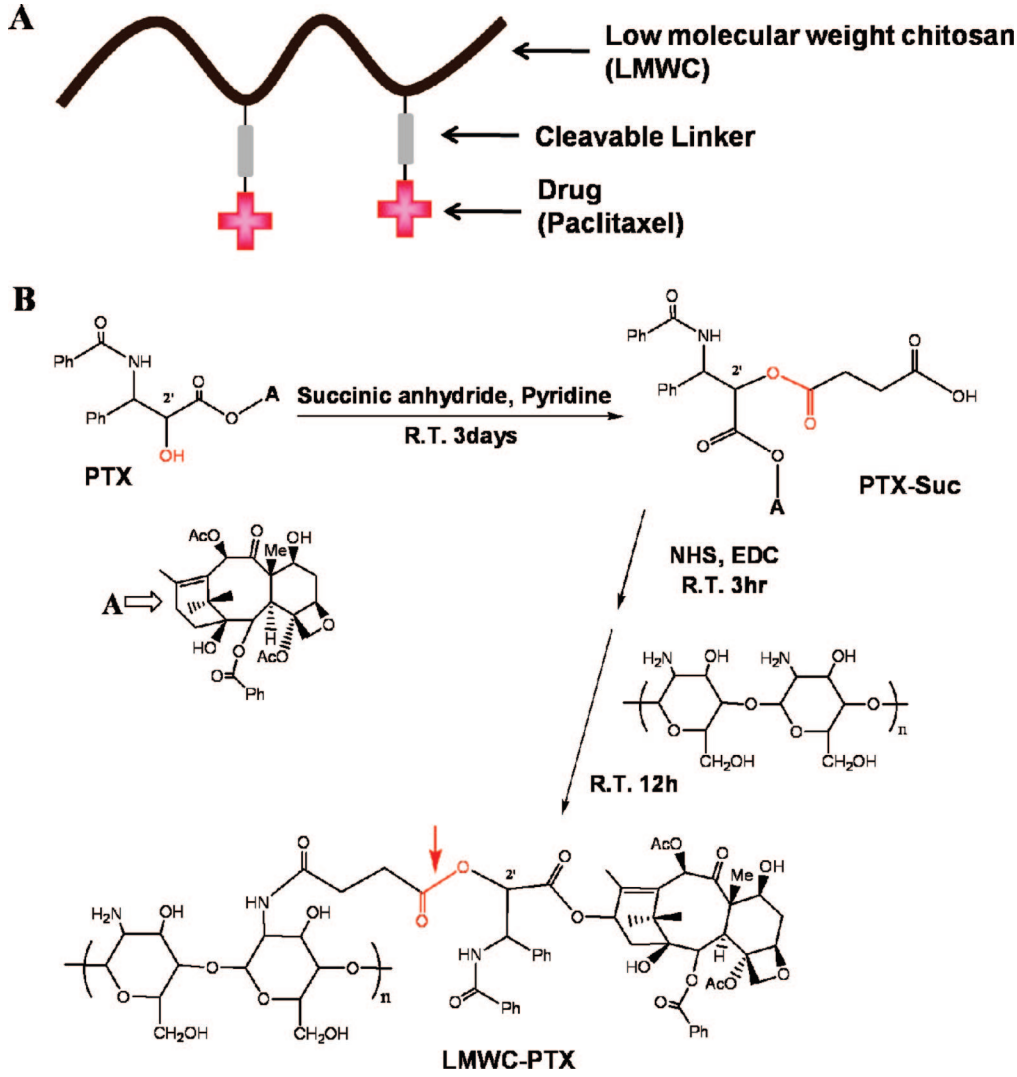

a narrow distribution of molecular weights so as to minimize fluctuation in the absorption and pharmacokinetic profiles of the conjugates. Within this context, we have examined the feasibility of using this conjugate system as a platform for oral delivery of PTX. In this report, we describe the synthesis, characterization, in vitro anticancer activity, pharmacokinetics, biodistribution, in vivo antitumor activity, and absorption mechanism of the LMWC-PTX conjugate.

Results and Discussion

Synthesis and Characterization of LMWC-PTX. A schematic illustration of the synthesis of LMWC-PTX conjugate is shown in Scheme 1. The drug molecules were covalently linked to LMWC through a succinate linker that is known to be cleaved to release a parent PTX drug under physiological conditions with hours of half-life.[35] LMWC-PTX was synthesized in a two-step process as seen in Scheme 1B: (i) modification of PTX with a succinic acid (the cleavable linker)[36] and (ii) coupling of the activated ester form of the succinic acid-modified PTX to the amine groups of LMWC under conditions.[37] The cleavable bond was indicated by an arrow in Scheme 1B. The formation of the conjugate was confirmed by ^{1}H NMR, which showed peaks corresponding to both LMWC and PTX (see Supporting Information, Figure S1). The UV spectrum of the conjugate obtained in a 50/50 (v/v) mixture of acetonitrile and water revealed that the conjugate was 12 ± 0.5 wt % PTX (see Supporting Information, Figure S2) and showed much greater water solubility (~1 mg/mL) than the native PTX (~0.03 mg/mL).

To verify that the linker was cleavable, we tested the stability of LMWC-PTX by incubating it in PBS (pH 7.4), simulated gastric fluid (SGF, pH 1.2), simulated intestinal fluid (SIF, pH 7.5), rat plasma, and cell culture medium (10% FBS) (Figure 1). While only ~2.4% and ~9.3% of PTX was released from the conjugate at 4 h post incubation in PBS and SGF, respectively, much higher amounts of drug release were observed for SIF (~17%), rat plasma (~25%), and cell culture medium (~51%). Considering that the transit time in the stomach is less than 4 h, the cleavage of the conjugate in SGF would seem insubstantial. Overall, this cleavage data implies that the conjugate would withstand the gastric environment but may be cleaved during or after uptake by the intestine and transport to the blood capillary, where the release of parent drug molecules mainly takes place.

In Vitro Cytotoxicity of LMWC-PTX. We next compared the in vitro anticancer activity of LMWC-PTX with that of parent PTX against human nonsmall cell lung cancer (NCI-H358), ovarian cancer (SK-OV-3), and breast cancer (MDA-

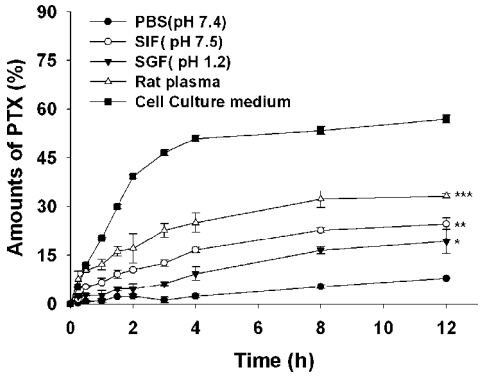

Figure 1. Stability assessment of LMWC-PTX with times upon incubation in PBS (pH 7.4), SIF (simulated intestinal fluid, pH 7.5), SGF (simulated gastric fluid, pH 1.2), rat plasma, and cell culture medium (10% FBS); bars, SE ($n = 3$). *$P < 0.05$, **$P < 0.01$, ***$P < 0.001$ vs PBS treated group.

MB-231) cells (see Supporting Information, Figure S3). We found that the two were similarly cytotoxic: the IC_{50} values against NCI-H358, SK-OV-3, and MDA-MB-231 were 3.8, 4.0, and 3.9 μg/mL for parent PTX and 5.1, 5.0, and 4.8 μg/mL for LMWC-PTX, respectively. We speculate that the similar cytotoxicity is attributed to a parent, active form of PTX released from the conjugate during the assay through cleavage of the succinate linker between the chitosan and PTX,[35] as the half-life of drug release from the conjugate in cell culture medium was about 4 h (Figure 1).

Pharmacokinetics and Biodistribution of LMWC-PTX. To access the pharmacokinetics of LMWC-PTX in vivo, we administered PTX (iv) formulated in cremophor EL/ethanol or LMWC-PTX (po) to normal ICR mice. The time-dependent clearance of LMWC-PTX from plasma is shown in Figure 2A,B. While PTX had a relatively short half-life in the plasma ($t_{1/2} \approx$ 1 h), the apparent half-life of LMWC-PTX was significantly longer ($t_{1/2} = 32$ h). The apparent bioavailability of LMWC-PTX at a dose of 10 mg and 5 mg PTX/kg was ~27% and 42% in comparison to that of 10 mg/kg PTX (iv), respectively; the value was ~54% and 86% in comparison to that of 5 mg/kg PTX (iv), respectively. It is still unclear, but this nonlinear relationship between bioavailability and dose is often found in the pharmacokinetics of PTX. To address this issue, we are planning to carry out more detailed and thorough pharmacokinetic studies using other animal species such as rats and dogs in the future preclinical development. We found that the pharmacokinetic profile of LMWC-PTX was similar to that obtained with 24 h of continuous iv infusion of PTX in humans.[38] It is also noteworthy that, unlike PTX (iv), the concentration of PTX remained above the required minimum therapeutic concentration (85.3 ng/mL)[39] over 48 h after administration of the conjugate (Figure 2A), which suggests that the present conjugate system could improve the therapeutic efficacy of cancer treatments with cell cycle-dependent drugs such as PTX. We speculate that these results reflect the transport of the intact conjugate into the blood stream and subsequent sustained release of the drug molecules through cleavage of the linker between LMWC and PTX.

We next used murine melanoma-bearing B16F10 mice to examine the uptake of orally administered LMWC-PTX by the tumor and compared the efficiency with that of intravenously injected PTX (iv). We found that the apparent PTX concentrations in tumor tissues were much higher in mice administered LMW-PTX than in those receiving PTX (iv), irrespective of the time of measurement (Figure 2C). For example, the PTX concentrations found in tumors 30 min after administration were 0.5 ± 0.1% and 2.4 ± 0.6% for PTX (iv) and LMWC-PTX (po), respectively, indicating a ~5-fold higher PTX uptake in the latter. Moreover, very similar PTX concentrations (2.24 ± 0.37%) were seen in tumors 24 h after administration of LMWC-PTX, a time when no PTX was detected in the tumors of mice administered PTX (iv). On the other hand, PTX (iv) showed much greater uptake by the liver and intestine than the conjugate, presumably because PTX is known to pass through the enterohepatic circulation and undergo first pass metabolism in those organs. Taken together, these results suggest that lower toxicity and higher antitumor efficacy can be anticipated with LMWC-PTX (po) than with PTX (iv).

In Vivo Antitumor Activity of LMWC-PTX. Encouraged by the high bioavailability and large tumor uptake of LMWC-PTX after oral administration, we next examined its in vivo antitumor efficacy using mice bearing murine melanomas (B16F10) or human nonsmall cell lung carcinomas (NCI-H358) as allograft and xenograft models, respectively (Figure 3). In the allograft model, we allowed the tumors to grow until their volumes were >50 mm^3, after which the mice ($n = 8$) were orally administered one of the following at the scheduled times: 25 mg/kg PTX, LMWC-PTX (25 mg PTX/kg, 184 mg/kg LMWC), 184 mg/kg LMWC, or saline (Figure 3A,B). Both the PTX and LMWC groups showed no statistically meaningful antitumor effects as compared to the control group (saline). By contrast, tumor growth was effectively suppressed in the LMWC-PTX group, resulting in ~86% inhibition relative to control (Figure 3A). This is likely indicative of the greater bioavailability and tumor uptake of the conjugate. We also measured body weights as an index of drug toxicity. The LMWC-PTX group, like the other groups, showed no appreciable loss in body weight for up to 23 d, indicating conjugation caused no additional toxicity.

In the xenograft tumor model, tumors were allowed to grow to an average volume of 150 mm^3 before treatment with one of the followings: PTX (iv) (formulated in cremophor EL/ethanol; 10 mg PTX/kg), which served as a positive control; LMWC-PTX (po, 10 mg PTX/kg), LMWC (po, 73 mg/kg); and saline (po), which served as a negative control (Figure 3C,D). PTX (iv) and LMWC-PTX effectively suppressed tumor growth by ~80% and 66%, respectively, whereas LMWC itself showed no antitumor activity. Considering that equivalent doses of PTX (10 mg/kg) were used in the conjugate and PTX (iv), the observed antitumor efficacy of the conjugate can be regarded as sufficiently high to warrant a clinical study. Furthermore, it should be noted that, unlike the PTX (iv) group, which showed a rapid decrease in the body weight, the LMWC-PTX group did not show an appreciable reduction in body weight, as compared to control (Figure 3D). This suggests that orally administered LMWC-PTX likely has advantages over the current clinical formulation of PTX, as it would eliminate the use of Cremophor EL, increase patient compliance, and may be more cost-effective in that it eliminates the need for hospitalization.

Mechanism of LMWC-PTX Absorption. To better understand the mechanism by which LMWC-PTX is absorbed, we first determined where the conjugate adheres within the GI tract by synthesizing a rhodamine-labeled LMWC conjugate (LMWC-Rhodamine), which we assumed would have characteristics similar to those of LMWC-PTX. Figure 4A shows an overlay of transmission and fluorescence images of ileum taken after oral administration of saline, LMWC, rhodamine, or LMWC-Rhodamine to ICR mice. While the rhodamine dye itself showed some nonspecific absorption throughout the small intestine,

A

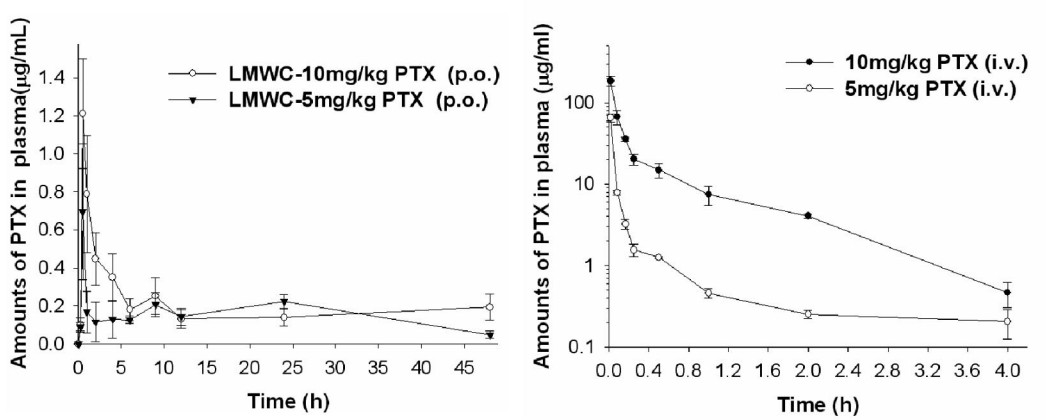

B

Parameters	PTX		LMWC-PTX	
	10mg/kg (i.v.)	5mg/kg (i.v.)	10mg/kg (p.o.)	5mg/kg (p.o.)
C_{max} (μg/mL)	-	-	1.21	0.70
T_{max} (hour)	-	-	0.5	0.5
Half life (hour)	0.56	0.68	33.86	31.05
AUC_{0-48} (μg*hr/mL)	35.32	8.72	9.47	7.47
Bioavailability (%)	100	100	26.81	85.70

C

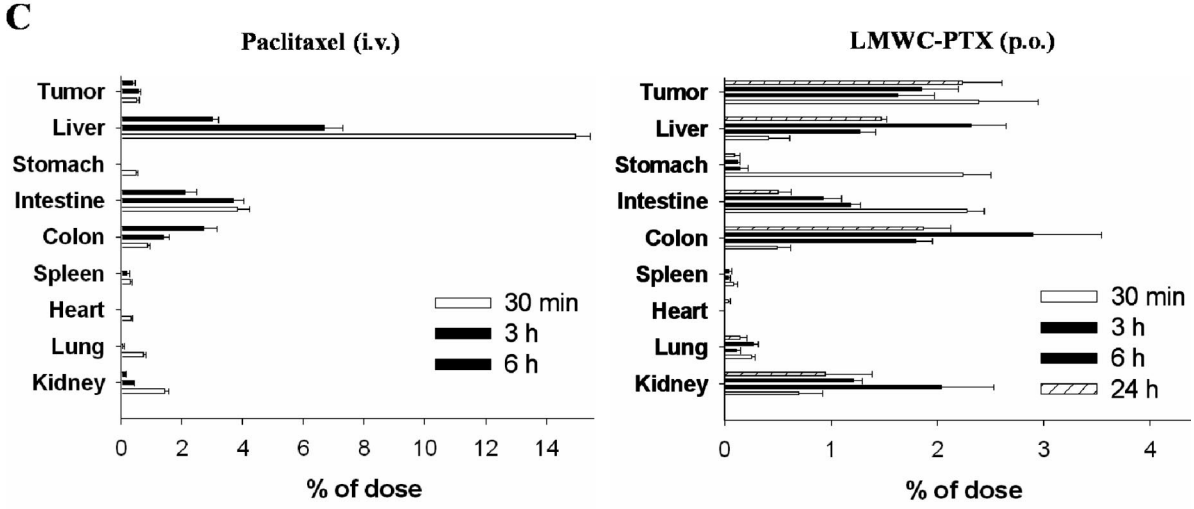

Figure 2. Dose-dependent plasma concentration of PTX (A), pharmacokinetic parameters (B), and tissue distribution of PTX (C) after administration of formulated PTX (iv) and LMWC-PTX (po), respectively; bars, SE ($n = 5$).

including the duodenum, jejunum (data not shown), and ileum, the fluorescent signal from LMWC-Rhodamine was seen exclusively in the ileum. In addition, unlike rhodamine, significant amounts of LMWC-Rhodamine were observed on both the surface of microvilli (lumenal side) and on the serosal side of the ileal epithelium. This suggests that the conjugate was able to adhere within the GI tract, particularly in the ileum, and then be transported across the epithelial layers.

To further verify that LMWC-PTX is absorbed from the GI tract, we prepared I^{125}-labeled LMWC-PTX and administered it to ICR mice. Figure 4B shows the time-dependent changes in the level of radioactivity detected in blood and several major organs after oral administration of the radiolabeled conjugate. Surprisingly, over half (~53% relative radioactivity) of the initial dose was detected in blood within 30 min after administration, and the remainder was found exclusively in the small intestine. Moreover, radioactivity levels were much higher in the ileum than duodenum or jejunum, which is in good agreement with the results obtained with the LMWC-Rhodamine. We also found it interesting that little radioactivity was detected in any other organs, including the lung, heart, spleen, and stomach, although low levels were detected in the liver. On the other hand, substantially decreased radioactivity was detected in blood with I^{125}-labeled LMWC compared to the conjugate (~17% vs 53%). This fact together with the pharmacokinetics of the conjugate suggests that LMWC-PTX is absorbed mostly in its intact conjugate form until it reaches the blood stream, where parent PTX is released.

We next investigated the effect of P-gp, which represents a major barrier to effective oral absorption of a variety of drugs, including PTX, and the effects of two major drug metabolic enzymes (Figure 4C,D) on LMWC-PTX absorption. The effect

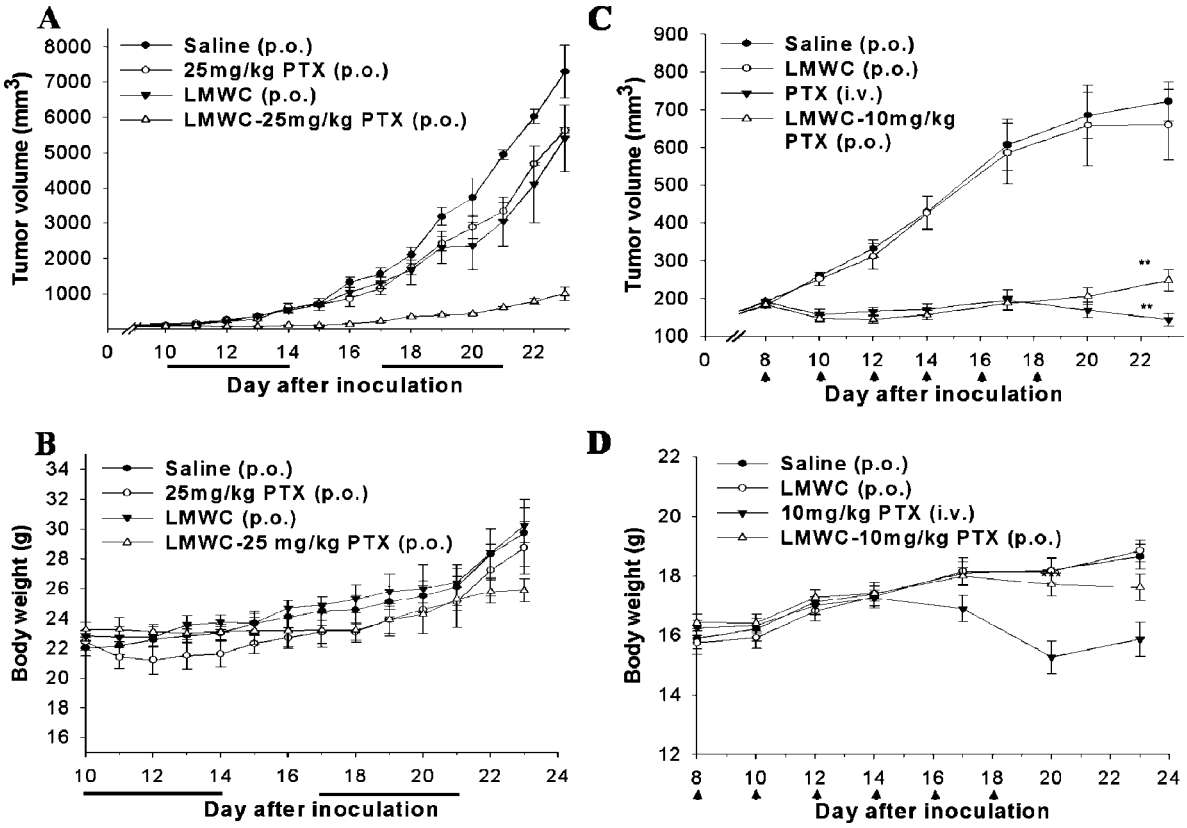

Figure 3. Antitumor efficacy of LMWC-PTX in mice bearing B16F10 murine melanoma (A,B) or NCI-H358 human nonsmall cell lung cancer (C,D). (A) Drugs were administered orally on the indicted schedules (solid lines); bars, SE ($n = 8$). $^{**}P < 0.01$ vs saline control. (B) Body weight changes in B16F10 tumor-bearing mice after oral administration; bars, SE ($n = 8$). (C) PTX was injected iv, and saline, LMWC, and LMWC-PTX were administered orally at the indicated times (arrowheads); bars, SE ($n = 8-12$). $^{**}P < 0.01$ vs saline control. (D) Body weight changes in NCI-H358 tumor-bearing mice after drug treatment; bars, SE ($n = 8-12$). $^{***}P < 0.001$ vs saline control.

of P-gp on the absorption of PTX and LMWC-PTX was evaluated in pharmacokinetic studies after oral administration of each compound with or without cyclosporine A, a commonly used P-gp inhibitor. As expected, coadministration of PTX (20 mg/kg) with cyclosporine A significantly increased the plasma PTX concentration, thereby increasing the bioavailability ~9-fold, from 0.23% to 2.1%. By contrast, we observed a slight reduction in the bioavailability of PTX, from 37% to 29%, when LMWC-PTX (20 mg PTX/kg) was administered together with cyclosporine A. This suggests LMWC-PTX is absorbed in a P-gp-independent manner, avoiding the undesired P-gp-mediated efflux of the drug in GI tract. In addition, the metabolic stability of LMWC-PTX and free PTX were compared using competitive inhibition assay kits (Figure 4D). PTX and positive controls both competitively inhibited the binding of a fluorescent substrate to CYP2C8, whereas LMWC-PTX had a much higher IC_{50}. In other words, the conjugate had a much lower affinity for the enzyme, suggesting it may bypass CYP-dependent drug metabolism, leading to greater oral bioavailability.

In summary, we have developed a new platform for oral delivery of PTX using a chemical conjugate system comprised of PTX and LMWC with a narrow molecular weight distribution (average MW: 6 kDa). This prodrug form of PTX is absorbed in the small intestine after oral administration and effectively inhibits tumor growth with an efficacy comparable to the clinically available injected form, but with much lower toxicity. The strong antitumor activity of LMWC-PTX after oral administration may be attributable to its greater water solubility, prolonged retention in the GI tract, and ability to bypass P-gp efflux pumps in the GI tract and CYP 450-dependent metabolism in intestine and liver. Taken together, we suggest this LMWC-based conjugate system may also be a useful tool for oral delivery of other poorly water-soluble drugs.

Experimental Section

Chemicals, Cells, and Animals. Paclitaxel (PTX) was purchased from Samyang Genex (Seoul, Korea). Low molecular weight chitosan (LMWC, average MW: 6 kDa) was from KITTOLIFE (Seoul, Korea) and was further purified by ultrafiltration. *N*-succinimidyl 3-(4-hydroxy, 5-[^{125}I] iodophenyl)-propionate (Bolton & Hunter reagent) was from Amersham Biosciences (Uppsala, Sweden). All other solvents and reagents were from Sigma Chemical (St. Louis, MO), were of reagent-grade, and were used as received. Cell lines were obtained from Korean Cell Line Bank (KCLB, Seoul, Korea) and were cultured according to the instructions from KCLB. All animals were obtained from Orient Bio Inc. (Seoul, Korea) and handled in accordance with the guidelines of the Animal Care and Use Committee in Gwangju Institute of Science and Technology.

Synthesis and Characterization of LMWC-PTX. A 2′-hemisuccinate derivative (PTX-Suc) of PTX was prepared by the previously reported method with some modifications.[37] Briefly, PTX (300 mg, 0.351 mmol) and succinic anhydride (46 mg, 1.3 equiv) were dissolved in CH_2Cl_2 (14 mL) at ambient temperature. After pyridine (39 μL, 1.37 equiv) was added, the mixture was vigorously stirred for 3 days at ambient temperature. The reaction mixture was concentrated in vacuum and loaded on silica gel column chromatography for purification. The purified PTX-Suc was obtained as white solid in 78% yield.

PTX-Suc (100 mg, 0.1 mmol) dissolved in anhydrous DMF (2 mL) was activated by *N*-hydroxy succiimide (NHS, 5 equiv) and 1-ethyl-3-(3-dimethylaminopropyl carbodiimide hydrochloride) (EDC, 1.1 equiv) for 4 h at room temperature to afford an NHS ester form of PTX-Suc. Subsequently, the resulting mixture was added to a

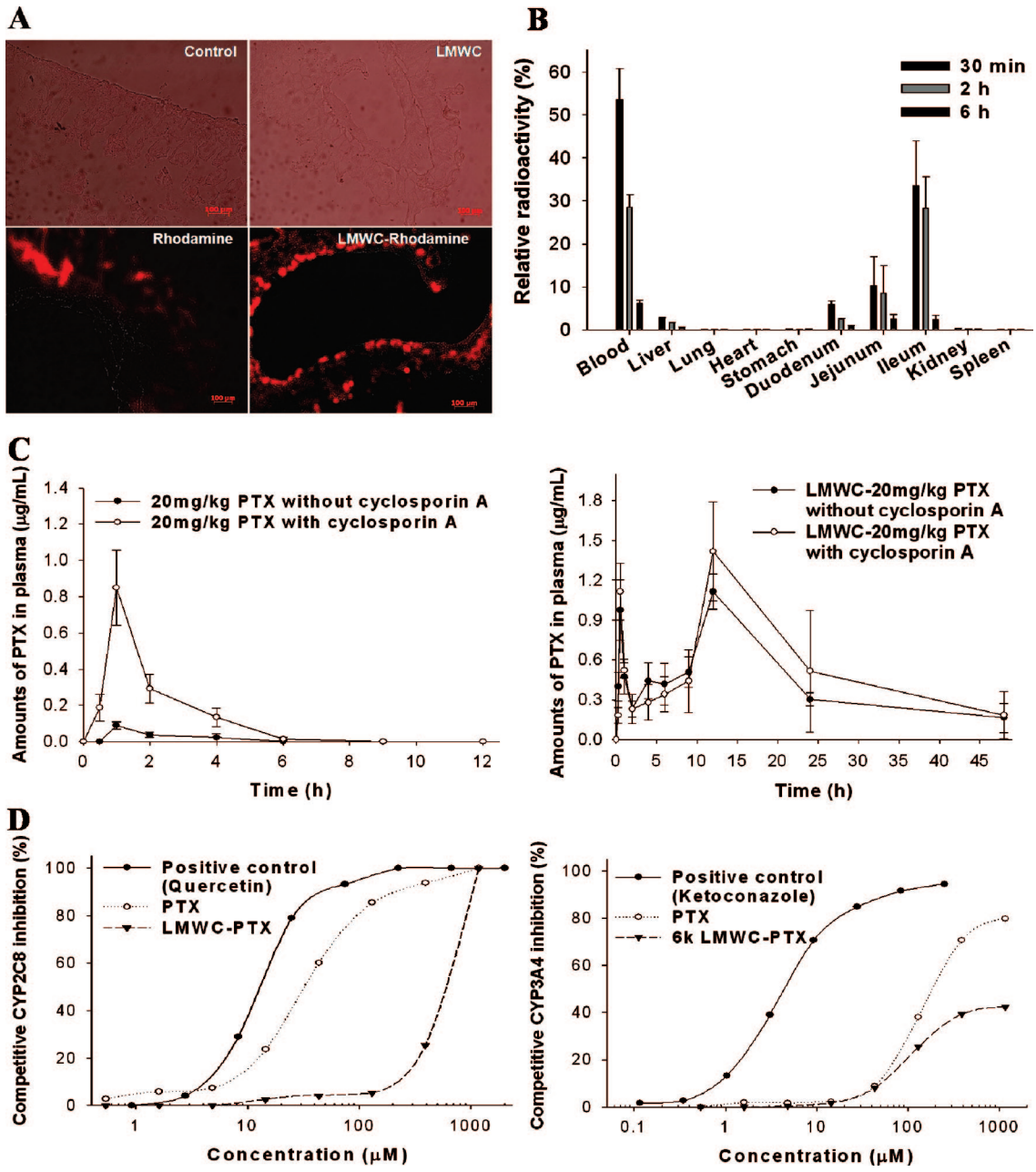

Figure 4. Mechanism of LMWC-PTX absorption. (A) Confocal laser scanning microscopy images of LMWC-Rhodamine. (B) Biodistribution of I^{125}-labeled LMWC-PTX (10 mg/kg PTX) after oral administration; bars, SE ($n = 3$). (C) Effect of P-gp inhibition (cyclosporin A, 15 mg/kg) after oral administration of 20 mg/kg PTX or LMWC-PTX (20 mg/kg PTX); bars, SE ($n = 4-5$). (D) Metabolic stability of LMWC-PTX in the presence of CYP450-dependent enzymes.

LMWC (157 mg, 0.025 equiv) in borate buffer (pH 10). After stirring for 12 h at room temperature, the reaction mixture was diluted by distilled water (5×) and extracted by ethyl ether (3 times) to remove unreacted PTX. The aqueous layer was dialyzed against distilled water using a dialysis membrane (MW cut off size: 3000), after which LMWC-PTX was lyophilized into white solid.

PTX-Suc: ^{1}H NMR (Xeol, 300 MHz, $CDCl_3$): δ1.11 [s, $^{17}CH_3$], 1.20 [s,$^{16}CH_3$], 1.69 [s, $^{19}CH_3$], 1.9 [s, $^{18}CH_3$], 2.2 [m, OAc], 2.4 [m, OAc], 2.5−2.8 [m, HOOC-CH_2CH_2-COO-TXL], 3.78 [d, ^{3}CH], 4.17 [d, $^{20}CH_2$], 4.3 [d, $^{20}CH_2$], 4.46 [dd, ^{7}CH], 4.96 [d, ^{5}CH], 5.50 [d, $^{2'}$CH], 5.67 [d,^{2}CH], 5.98 [dd, $^{3'}$CH], 6.22 [t, ^{13}CH], 6.27 [s, ^{10}CH], 7.09 [d, NH], 7.25 [s, 3′-Ph], 7.4 [m, 3′-NBz], 7.5 [m, 2-OBz], 7.73 [d, 3′-NBz], 8.1 [d, 2-OBz].

Measurement of Solubility of LMWC-PTX. Water solubility of LMWC-PTX conjugate was measured as described elsewhere.[36] Briefly, the conjugate (16.6 mg) was dissolved in 1.0 mL of D_2O with sonication for 15 min. The resulting mixture was centrifuged for 20 min to remove the undissolved conjugate. The supernatant solution was analyzed by ^{1}H NMR spectroscopy to confirm the presence of the conjugate and then was further analyzed by UV−vis spectroscopy to obtain the concentration of the conjugate.

Stability Study of LMWC-PTX. Stability studies were carried out in PBS (pH 7.4), simulated intestinal fluid containing 1% pancreatin (SIF, pH 7.5), simulated gastric fluid containing 0.32% pepsin (SGF, pH 1.2), rat plasma, and cell culture medium (10% FBS) at 37 °C for up to 12 h. The conjugate (5 mg) was dissolved in 2.5 mL of each fluid, after which 100 μL of samples were taken at given times. The free PTX was then extracted by using 1 mL of ethyl acetate. Released free PTX was measured by reverse-phase high-performance liquid chromatography (HPLC; Shimadzu, Kyoto, Japan) on a C_{18} column (300 mm × 3.9 mm Nova-Pak Waters) with acetonitrile/water. The significance of differences in the uptake levels between groups was assessed using Student's *t*-test.

Pharmacokinetic and Biodistribution Studies. Normal female ICR mice (25−30 g) were administered 10 mg/kg of PTX (iv) formulated in cremophor EL/ethanol via the tail vein. Mice used for oral administration were fasted for 12 h and then administered a single oral dose of LMWC-PTX (5 or 10 mg of equivalent PTX/kg) through a blunt needle that was passed down the esophagus into the stomach. The LMWC-PTX solution was prepared in a 10% DMSO solution, and the total volume of the administered LMWC-PTX solution was 300 μL. For subsequent analyses, blood (450 μL) was collected from a capillary in the retro-orbital plexus and mixed with 50 μL of sodium citrate (3.8% solution), after which the sample was immediately centrifuged at 800*g* for 20 min. The PTX was then extracted from 100 μL of plasma using 1 mL of ethyl acetate. The extraction efficiency for PTX was 95%. The samples were then centrifuged for 10 min at 35000*g*, after which the supernatant was separated and dried. The dried extract was reconstituted with 1 mL of HPLC mobile phase, and a 50-μL aliquot was injected into the HPLC for determination of free PTX. Pharmacokinetic parameters were analyzed based on a noncompartmental model using Microsoft Excel.[40]

In a separate experiment, C57BL6 mice bearing B16F10 murine melanomas (100 mm^3) were administered 10 mg PTX/kg of formulated PTX (iv) via the tail vein or LMWC-PTX (po). Then 3, 6, 9, 12, and 24 h after injection or oral administration, mice were sacrificed and the liver, stomach, intestine, colon, spleen, kidney, lung, heart, and tumor were excised. After weighting each tissue, 5 mL of acetonitrile was added and the tissue was homogenized. The homogenates were centrifuged at 20000*g* for 10 min, after which 500 μL of the supernatant was collected and added to 500 μL of water. Aliquots (50 μL) of the reconstituted samples were then injected into an HPLC for determination of free PTX.

In Vivo Antitumor Activity. To estimate the antitumor effect of LMWC-PTX against allografts, tumors were induced in female C57BL6 mice (20−25 g) by sc inoculation of approximately 1×10^5 murine melanoma (B16F10) cells into their backs. When the tumors were at least 50 mm^3 in size, PTX or LMWC-PTX was administered orally at 25 mg/kg/day for two 5-day cycles separated by a 2-day interval.

To assess the antitumor effect of LMWC-PTX against xenografts, tumors were induced in female athymic nude (NCR *nu/nu*) mice (20−25 g) by sc inoculation of approximately 6×10^6 human nonsmall cell lung cancer (NCI-H358) cells. When the tumors were at least 150 mm^3 in size, the mice were administered 10 mg/kg/day formulated PTX (iv) or LMWC-PTX (10 mg PTX/kg/day) (po) every other day until six doses had been given. Control mice were administered saline, LMWC solution. Tumor volumes were measured using calipers and calculated using the equation $(^1/_2)$ $(L \times W^2)$. The significance of the difference in uptake levels between groups was assessed using Student's *t*-test.

Assessment of the Site of Conjugate Absorption in GI Tract Using LMWC-Rhodamine. LMWC-Rhodamine was synthesized from LMWC and 5(6)-carboxytetramethylrhodamine *N*-succinimidyl ester (BioChemiac) under similar conditions as LMWC-PTX. Briefly, the rhodamine derivative (8.4 mg, 15.9 μmol) dissolved in DMF (1 mL) was added to a solution of LMWC (47.7 mg, 7.6 μmol) in water (0.8 mL)/DMF (1.6 mL) and the reaction mixture was stirred for 8 h at room temperature. Then unbound rhodamine was eliminated by extraction using ethyl acetate (×3) and the conjugate was further purified by dialysis using a cellulose membrane with MWCO 1000 for 1 day. The content of rhodamine in the conjugate was quantified by fluorescence measurement using a fluorescence spectrometer (RF-5301PC, Shimadzu, Japan) at an excitation and emission wavelength of 543 and 576 nm, respectively.

Absorption experiment of LMWC-Rhodamine was carried out as follows. A rhodamine derivative (20 mg/kg), LMWC (184 mg/kg), and LMWC-Rhodamine (204 mg/kg) were orally administered to ICR mice (25−30 g). After 30 min and 1 h, mice were euthanized and then duodenum, jejunum, and ileum of each mouse were collected. Several parts of the collected tissues were laid onto the OCT in the mold for fixation and stored at −70 °C. Thin tissue sections were then prepared by using a microtome (Leica RM2245, Wetzlar, Germany), and the distributions of the rhodamine derivative and LMWC-Rhodamine were assessed using a fluorescence microscope (Axiovert 200M, ZEISS, Germany).

Biodistribution Study Using I^{125}-Labeled LMWC-PTX. LMWC-PTX was radiolabeled using I^{125}-labeled Bolton−Hunter reagent (BHR). Briefly, LMWC-PTX (12 μg, 2 nmol) dissolved in a borate buffer (6 μL) was added to a solution of I^{125}-labeled Bolton−Hunter reagent (0.2 nmol, 80 μL, 400 μCi) and the reaction mixture was stirred for 3 h at room temperature. After reaction, the unbound BHR was removed by extraction using ethyl acetate (×3) and the radiolabeled conjugate was purified by dialysis using a cellulose membrane of MWCO 1000 for 6 h. The content of I^{125} in the conjugate was measured by using a gamma counter (1480 Wizard3, PerkinElmer, Inc.). ^{125}I-labeled LMWC-PTX (38 nCi) was then orally administered to ICR mice (25−30 g). Then 0.5, 2, and 6 h after administration, blood was collected, mice were sacrificed, and the liver, stomach, intestine, colon, spleen, kidney, lung, heart, and tumor were excised and the tissue-associated radioactivity was determined using a gamma counter. The radioactivity in the mouse tissues was expressed as a percentage of administered doses. Uptake levels were expressed as % administered-dose per each organ.

Effect of a P-gp Inhibitor on LMWC-PTX Absorption. To estimate effects of P-gp on absorption, ICR mice (25−30 g) were fasted for 12 h before oral administration of 10 mg/kg PTX or LMWC-PTX (10 mg/kg PTX equivalent) using a blunt needle via the esophagus into the stomach. When administering a P-gp inhibitor, the oral solution also contained 15 mg/kg cyclosporine A. Blood samples were subsequently collected from the retro-orbital vein and centrifuged for 20 min at 3000*g*, after which plasma PTX concentrations were determined by HPLC.

To assess metabolism by CYP450-dependent enzymes, CYP450 inhibition assays were conducted using a High Throughput Inhibitor Screening Kit (HTS Kit, BD GENTEST).[41] These assays enabled us to monitor, via fluorescence detection, metabolite formation following incubation of the CYP enzyme with a specific substrate. PTX and LMWC-PTX were tested with CYP3A4 and CYP2C8, as these enzymes had been shown to exhibit inhibition. Reactions were run in 96-well plates at 37 °C. Inhibition of metabolic product formation from the test compound was tested for each enzyme in the absence and presence of the test compound. The amount of metabolic product formed was quantified using a fluorescence plate reader with excitation and emission filters that were optimized for detection of each metabolite.

Acknowledgment. This work was supported by the Cell Dynamics Research Center, Korean Ministry of Science and Technology.

Supporting Information Available: ^{1}H NMR, UV spectra, and cytotoxicity data in vitro of the LMWC-PTX conjugate. This material is available free of charge via the Internet at http://pubs.acs.org.

References

(1) Rowinsky, E. K.; Donehower, R. C. Paclitaxel (Taxol). *N. Engl. J. Med.* **1995**, *332*, 1004–1014.

(2) Adams, J. D; Flora, K. P.; Goldspiel, B. R.; Wilson, J. W.; Arbuck, S. G.; Finley, R. Taxol: a history of pharmaceutical development current pharmaceutical concerns. *J. Natl. Cancer Inst. Monogr.* **1993**, *15*, 141–147.

(3) Weiss, R. B.; Donehower, R. C.; Wiernik, P. H.; Ohnuma, T.; Gralla, R. J.; Trump, D. L.; Baker, J., Jr.; Van Echo, D. A.; Von Hoff, D. D.; Leyland-Jones, B. Hypersensitivity reactions from Taxol. *J. Clin. Oncol.* **1990**, *8*, 1263–1268.

(4) Sparreboom, A.; van Tellingen, O.; Nooijen, W. J.; Beijnen, J. H. Nonlinear pharmacokinetics of paclitaxel in mice results from the pharmaceutical vehicle Cremophor EL. *Cancer Res.* **1996**, *56*, 2112–2115.

(5) Ibrahim, N. K.; Desai, N.; Legha, S.; Soon-Shiong, P.; Theriault, R. L.; Rivera, E.; Esmaeli, B.; Ring, S. E.; Bedikian, A.; Hortobagyi, G. N.; Ellerhorst, J. A. Phase I and pharmacokinetic study of ABI-007, a Cremophor-free, protein-stabilized, nanoparticle formulation of paclitaxel. *Clin. Cancer Res.* **2002**, *8*, 1038–1044.
(6) Kim, T. Y.; Kim, D. W.; Chung, J. Y.; Shin, S. G.; Kim, S. C.; Heo, D. S.; Kim, N. K.; Bang, Y. J. Phase I and pharmacokinetic study of Genexol-PM, a Cremophor-free, polymeric micelle-formulated paclitaxel, in patients with advanced malignancies. *Clin. Cancer Res.* **2004**, *10*, 3708–3716.
(7) Kim, J. H.; Kim, Y. S.; Kim, S.; Park, J. H.; Kim, K.; Choi, K.; Chung, H.; Jeong, S. Y.; Park, R. W.; Kim, I. S.; Kwon, I. C. Hydrophobically modified glycol chitosan nanoparticles as carriers for paclitaxel. *J. Controlled Release* **2006**, *111*, 228–234.
(8) van Vlerken, L. E.; Duan, Z.; Seiden, M. V.; Amiji, M. M. Modulation of Intracellular Ceramide Using Polymeric Nanoparticles to Overcome Multidrug Resistance in Cancer. *Cancer Res.* **2007**, *67*, 4843–4850.
(9) Safavy, A. Recent developments in taxane drug delivery. *Curr. Drug Delivery* **2008**, *5*, 42–54.
(10) Bae, K. H.; Lee, Y.; Park, T. G. Oil-encapsulating PEO-PPO-PEO/PEG shell cross-linked nanocapsules for target-specific delivery of paclitaxel. *Biomacromolecules* **2007**, *8*, 650–656.
(11) Lee, I. H.; Park, Y. T.; Roh, K.; Chung, H.; Kwon, I. C.; Jeong, S. Y. Stable paclitaxel formulations in oily contrast medium. *J. Controlled Release* **2005**, *102*, 415–425.
(12) Yang, S.; Gursoy, R. N.; Lambert, G.; Benita, S. Enhanced oral absorption of paclitaxel in a novel self-microemulsifying drug delivery system with or without concomitant use of P-glycoprotein inhibitors. *Pharm. Res.* **2004**, *21*, 261–270.
(13) Li, C.; Yu, D. F.; Newman, R. A.; Cabral, F.; Stephens, L. C.; Hunter, N.; Milas, L.; Wallace, S. Complete regression of well-established tumors using a novel water-soluble poly(L-glutamic acid)−paclitaxel conjugate. *Cancer Res.* **1998**, *58*, 2404–2409.
(14) Duncan, R. Polymer conjugates as anticancer nanomedicines. *Nat. Rev. Cancer* **2006**, *6*, 688–701.
(15) Vicent, M. J.; Duncan, R. Polymer conjugates: nanosized medicines for treating cancer. *Trends Biotechnol.* **2006**, *24*, 39–47.
(16) Sugahara, S.; Kajiki, M.; Kuriyama, H.; Kobayashi, T. R. Complete regression of xenografted human carcinomas by a paclitaxel−carboxymethyl dextran conjugate (AZ10992). *J. Controlled Release* **2007**, *117*, 40–50.
(17) Bradley, M. O.; Webb, N. L.; Anthony, F. H.; Devanesan, P.; Witman, P. A.; Hemamalini, S.; Chander, M. C.; Baker, S. D.; He, L.; Horwitz, S. B.; Swindell, C. S. Tumor targeting by covalent conjugation of a natural fatty acid to paclitaxel. *Clin. Cancer Res.* **2001**, *7*, 3229–3238.
(18) Xie, Z.; Guan, H.; Chen, X.; Lu, C.; Chen, L.; Hu, X.; Shi, Q.; Jing, X. A novel polymer−paclitaxel conjugate based on amphiphilic triblock copolymer. *J. Controlled Release* **2007**, *117*, 210–216.
(19) Polizzi, D.; Pratesi, G.; Tortoreto, M.; Supino, R.; Riva, A.; Bombardelli, E.; Zunino, F. A novel taxane with improved tolerability and therapeutic activity in a panel of human tumor xenografts. *Cancer Res.* **1999**, *59*, 1036–1040.
(20) Rautio, J.; Kumpulainen, H.; Heimbach, T.; Oliyai, R.; Oh, D.; , T.; Savolainen, J. Prodrugs: design and clinical applications. *Nat. Rev. Drug Discovery* **2008**, *7*, 255–270.
(21) Skwarczynski, M.; Hayashi, Y.; Kiso, Y. Paclitaxel prodrugs: toward smarter delivery of anticancer agents. *J. Med. Chem.* **2006**, *49*, 7253–7269.
(22) Zou, Y.; Fu, H.; Ghosh, S.; Farquhar, D.; Klostergaard, J. Antitumor activity of hydrophilic paclitaxel copolymer prodrug using locoregional delivery in human orthotopic nonsmall cell lung cancer xenograft models. *Clin. Cancer Res.* **2004**, *10*, 7382–7391.
(23) Greenwald, R. B.; Gilbert, C. W.; Pendri, A.; Conover, C. D.; Xia, J.; Martinez, A. Drug delivery systems: water soluble taxol 2′-poly(ethylene glycol) ester prodrugs−design and in vivo effectiveness. *J. Med. Chem.* **1996**, *39*, 424–431.
(24) Choi, J. S.; Shin, S. C. Enhanced paclitaxel bioavailability after oral coadministration of paclitaxel prodrug with naringin to rats. *Int. J. Pharm.* **2005**, *292*, 149–156.
(25) O'Neill, V. J.; Twelves, C. J. Oral cancer treatment: developments in chemotherapy and beyond. *Br. J. Cancer* **2002**, *87*, 933–937.
(26) Malingré, M. M.; Beijnen, J. H.; Schellens, J. H. Oral delivery of taxanes. *Invest. New Drugs* **2001**, *19*, 155–162.
(27) Meerum Terwogt, J. M.; Malingré, M. M.; Beijnen, J. H.; ten Bokkel Huinink, W. W.; Rosing, H.; Koopman, F. J.; van Tellingen, O.; Swart, M.; Schellens, J. H. Coadministration of oral cyclosporin A enables oral therapy with paclitaxel. *Clin. Cancer Res.* **1999**, *5*, 3379–3384.
(28) Nicoletti, M. I.; Colombo, T.; Rossi, C.; Monardo, C.; Stura, S.; Zucchetti, M.; Riva, A.; Morazzoni, P.; Donati, M. B.; Bombardelli, E.; D'Incalci, M.; Giavazzi, R. IDN5109, a Taxane with oral bioavailability and potent antitumor activity. *Cancer Res.* **2000**, *60*, 842–846.
(29) Hong, J. W.; Lee, I. H.; Kwak, Y. H.; Park, Y. T.; Sung, H. C.; Kwon, I. C.; Chung, H. Efficacy and tissue distribution of DHP107, an oral paclitaxel formulation. *Mol. Cancer Ther.* **2007**, *6*, 3239–3247.
(30) Cabot, M. C.; Giuliano, A. E.; Han, T. Y.; Liu, Y. Y. SDZ PSC 833, the Cyclosporine A analogue and multidrug resistance modulator, activates ceramide synthesis and increases vinblastine sensitivity in drug-sensitive and drug-resistant cancer cells. *Cancer Res.* **1999**, *59*, 880–885.
(31) Ueda, K.; Cardarelli, C.; Gottesman, M. M.; Pastan, I. Expression of a full-length cDNA for the human "MDR1" gene confers resistance to colchicine, doxorubicin, and vinblastine. *Proc. Natl. Acad. Sci. U.S.A.* **1987**, *84*, 3004–3008.
(32) Thanou, M.; Verhoef, J. C.; Junginger, H. E. Oral drug absorption enhancement by chitosan and its derivatives. *Adv. Drug Delivery Rev.* **2001**, *52*, 117–126.
(33) Kumar, M. N.; Muzzarelli, R. A.; Muzzarelli, C.; Sashiwa, H.; Domb, A. J. Chitosan chemistry and pharmaceutical perspectives. *Chem. Rev.* **2004**, *104*, 6017–6084.
(34) Chae, S. Y.; Jang, M. K.; Nah, J. W. Influence of molecular weight on oral absorption of water soluble chitosans. *J. Controlled Release* **2005**, *102*, 383–394.
(35) Safavy, A.; Georg, G. I.; Vander Velde, D.; Raisch, K. P.; Safavy, K.; Carpenter, M.; Wang, W.; Bonner, J. A.; Khazaeli, M. B.; Buchsbaum, D. J. Site-specifically traced drug release and biodistribution of a paclitaxel−antibody conjugate toward improvement of the linker structure. *Bioconjugate Chem.* **2004**, *15*, 1264–1274.
(36) Nicolaou, K. C.; Riemer, C.; Kerr, M. A.; Rideout, D.; Wrasidlo, W. Design, synthesis and biological activity of protaxols. *Nature* **1993**, *364*, 464–466.
(37) Thierry, B.; Kujawa, P.; Tkaczyk, C.; Winnik, F. M.; Bilodeau, L.; Tabrizian, M. Delivery platform for hydrophobic drugs: prodrug approach combined with self-assembled multilayers. *J. Am. Chem. Soc.* **2005**, *127*, 1626–1627.
(38) Wiernik, P. H.; Schwartz, E. L.; Einzig, A.; Strauman, J. J.; Lipton, R. B.; Dutcher, J. P. Phase I trial of taxol given as a 24-h infusion every 21 days: responses observed in metastatic melanoma. *J. Clin. Oncol.* **1987**, *5*, 1232–1239.
(39) Huizing, M. T.; Giaccone, G.; van Warmerdam, L. J.; Rosing, H.; Bakker, P. J.; Vermorken, J. B.; Postmus, P. E.; van Zandwijk, N.; Koolen, M. G.; ten Bokkel Huinink, W. W.; van der Vijgh, W. J.; Bierhorst, F. J.; Lai, A.; Dalesio, O.; Pinedo, H. M.; Veenhof, C. H.; Beijnen, J. H. Pharmacokinetics of paclitaxel and carboplatin in a dose-escalating and dose-sequencing study in patients with nonsmall-cell lung cancer. *J. Clin. Oncol.* **1997**, *15*, 317–329.
(40) Sato, H.; Sato, S.; Wang, Y. M.; Horikoshi, I. Add-in macros for rapid and versatile calculation of noncompartmental pharmacokinetic parameters on Microsoft Excel spreadsheets. *Comput. Methods Programs Biomed.* **1996**, *50*, 43–52.
(41) Labrie, P.; Maddaford, S. P.; Lacroix, J.; Catalano, C.; Lee, D. K.; Rakhit, S.; Gaudreault, R. C. In vitro activity of novel dual action MDR anthranilamide modulators with inhibitory activity at CYP-450. *Bioorg. Med. Chem.* **2006**, *14*, 7972–7987.

JM800767C